



Cite this: DOI: 10.1039/d6cp01378c

 Received 13th April 2026,  
Accepted 2nd June 2026

DOI: 10.1039/d6cp01378c

[rsc.li/pccp](https://rsc.li/pccp)

## Turning up chirality: hydrostatic pressure boosts circularly polarized luminescence in europium complexes

 Ayaka Miyoshi,<sup>a</sup> Hitoha Abe,<sup>b</sup> Honoka Akiyama,<sup>a</sup> Keisuke Yoshida<sup>a</sup> and Yoshitane Imai<sup>id</sup>\*<sup>a</sup>

**We examine the ability of hydrostatic pressure to directly influence intra- and intermolecular distances and chiral organisation. We investigate pressure-responsive circularly polarised luminescence in optically active europium complexes doped with axially chiral 2,2'-bis(diphenylphosphino)-1,1'-binaphthyl and point-chiral (R,R)-(-)-2,3-bis(tert-butylmethylphosphino)quinoxaline ligands. A new molecular design strategy for pressure-responsive sensing materials is described.**

Circularly polarised luminescence (CPL) is a photophysical phenomenon in which the photoexcitation of a chiral lumino-phore generates left-handed and right-handed circularly polarised light with unequal emission intensities. Owing to this intrinsic chiroptical asymmetry, CPL-active materials are attracting attention for application in next-generation displays, optical information processing and encryption, chiral sensing, and quantum photonics.<sup>1</sup> However, advancing functional CPL materials and developing high-performance CPL systems requires molecular design principles that enable the precise and reversible control of these parameters in response to external stimuli. CPL depends not only on the ground-state chirality of a molecule but also on intermolecular interactions, coordination environments, local symmetry, and electronic structures in the photoexcited state. Accordingly, constructing and reinforcing a chiral environment in the excited state through the introduction of chiral ligands, exploitation of host-guest interactions, or formation of chiral supramolecular assemblies are key strategies for enhancing CPL responses. In particular, lanthanide complexes occupy a central position in CPL research because they exhibit sharp line-like emissions and large luminescence dissymmetry factors (*g*-values).<sup>2</sup> In lanthanide complex systems, CPL properties are governed less by the

intrinsic nature of the metal centre itself than by the surrounding structural elements, such as the ligand arrangement, local symmetry, and solvation state. Therefore, the application of external stimuli capable of modulating the structure or symmetry of a complex without chemical modification is a highly promising approach for CPL control.<sup>3</sup>

Pressure has emerged as a promising external stimulus. Without altering the chemical composition, pressure enables the continuous and precise modulation of intermolecular distances, ligand arrangements, and even solvation structures. It offers a unique opportunity to control the chiral environment in the excited state in a nonthermal and potentially reversible manner. Pressure acts uniformly in solution systems and can reliably induce subtle structural changes in coordination complexes and their surrounding environments, making it an exceptionally powerful external parameter for elucidating the origin of CPL responses.<sup>4,5</sup>

In this study, we investigated a lanthanide complex solution system under dynamic equilibrium in the presence of chiral ligands. We also studied the effect of hydrostatic pressure on the modulation and amplification of CPL properties. Therefore, this study demonstrates the feasibility of pressure-responsive CPL control in lanthanide complexes and provides new design principles for chiral luminescent materials regulated by external fields.

The D<sub>3</sub>-symmetric Eu(III)(hfa)<sub>3</sub> complex (hfa = 1,1,1,5,5,5-hexafluoroacetylacetonate) possesses relatively weak steric constraints owing to the small size of the hfa ligands and undergoes rapid interconversion between the  $\Delta$  and  $\Lambda$  configurations in solution. As a result, the complex does not exist as a configurationally stable single enantiomer but rather as a racemic  $\Delta$ - $\Lambda$  mixture under dynamic equilibrium. In this study, we attempted to control the chiral environment in the excited state by introducing highly enantiopure chiral ligands into a dynamic equilibrium system. Specifically, axially chiral (*S*)-/(*R*)-2,2'-bis(diphenylphosphino)-1,1'-binaphthyl (BINAP) and centrally chiral (*S,S*)-/(*R,R*)-(-)-2,3-bis(tert-butylmethylphosphino)quinoxaline (QuinoxP) were selected as coordinating ligands and

<sup>a</sup> Graduate School of Science and Engineering, Kindai University, 3-4-1 Kowakae Higashi-Osaka, Osaka 577-8502, Japan

<sup>b</sup> Department of Applied Chemistry, Faculty of Science and Engineering, Kindai University, 3-4-1 Kowakae, Higashi-Osaka, Osaka 577-8502, Japan



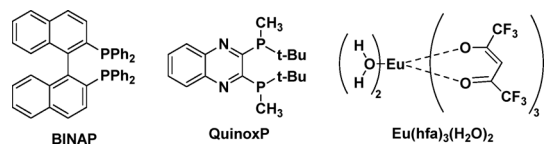


Fig. 1 Molecular structures of (*R*)- and (*S*)-BINAP, (*R,R*)- and (*S,S*)-QuinoxP, and  $\text{Eu}(\text{hfa})_3(\text{H}_2\text{O})_2$  (hfa = 1,1,1,5,5,5-hexafluoroacetylacetonate).

incorporated into the  $\Delta$ - $\Lambda$  mixed  $\text{Eu}(\text{III})(\text{hfa})_3$  system to construct emissive complexes (Fig. 1).

By comparing the ligands with distinct stereochemical characteristics (axial *versus* central chirality), a system was designed to elucidate correlations between the pressure responsiveness and chirality induction effects. The resulting chiral BINAP/ $\text{Eu}(\text{III})(\text{hfa})_3$  and QuinoxP/ $\text{Eu}(\text{III})(\text{hfa})_3$  emitters were subjected to optical characterisation under high-pressure conditions. Systematic analyses of pressure-dependent changes in PL and CPL emission maxima, emission intensities, and luminescence dissymmetry factors (*g*-values) enable the evaluation of the influence of hydrostatic pressure on the excited-state chiral environment and local symmetry around the  $\text{Eu}(\text{III})$  emissive centre.  $\text{Eu}(\text{hfa})_3(\text{H}_2\text{O})_2$  is synthesised from  $(\text{CH}_3\text{COO})_3\text{Eu}\cdot n\text{H}_2\text{O}$  and  $\text{CH}_2(\text{COCF}_3)_2$  according to a previously reported procedure.<sup>6</sup> The resulting complex is isolated with a 32% yield. The chiral emissive system is prepared by mixing (*R*)-BINAP (or (*S*)-BINAP) with  $\text{Eu}(\text{hfa})_3(\text{H}_2\text{O})_2$  in chloroform at a 1 : 1 molar ratio (Fig. 1). Ligand exchange in this solution produces the BINAP- $\text{Eu}(\text{III})(\text{hfa})_3$  complex, which is used directly for photophysical characterisation.

To evaluate the CPL response under high-pressure conditions, hydrostatic pressure is applied to a chloroform solution of the chiral emitter BINAP- $\text{Eu}(\text{III})(\text{hfa})_3$ , and the pressure-induced enhancement of CPL is examined. Emission measurements at ambient and elevated pressures are performed according to previously reported methods (SI and Fig. S1).<sup>5</sup> At ambient pressure (0.1 MPa), the CPL spectra of chiral (*R*)-BINAP- $\text{Eu}(\text{III})(\text{hfa})_3$  and (*S*)-BINAP- $\text{Eu}(\text{III})(\text{hfa})_3$  exhibit clear mirror-image relationships (yellow lines, Fig. 2 and Fig. S2). CPL emission maxima

( $\lambda_{\text{CPL}}$ ) are observed at 652, 612, 599, and 586 nm, corresponding to the characteristic  $\text{Eu}(\text{III})$  4*f*-4*f* transitions. These bands are assigned to the  $^5\text{D}_0 \rightarrow ^7\text{F}_J$  ( $J = 0-3$ ) transitions, respectively. The degree of circular polarisation in the excited state is commonly evaluated by the luminescence dissymmetry factor,  $g_{\text{CPL}}$ , defined as  $g_{\text{CPL}} = \Delta I/I = 2(\text{IL} - \text{IR})/(\text{IL} + \text{IR})$ , where IL and IR represent the emission intensities of the left- and right-circularly polarised light under unpolarised excitation. In the present system, the  $|g_{\text{CPL}}|$  values are  $6.2 \times 10^{-2}$  at 652 nm,  $5.4 \times 10^{-3}$  at 612 nm,  $9.4 \times 10^{-3}$  at 599 nm, and  $1.3 \times 10^{-2}$  at 586 nm. Notably, a relatively large *g*-value is obtained at 652 nm, suggesting a pronounced contribution from the coordination-induced local symmetry breaking around the  $\text{Eu}(\text{III})$  centre. Unmodified  $\text{Eu}(\text{III})(\text{hfa})_3$  exists in solution as a dynamic equilibrium mixture of the  $\Delta$  and  $\Lambda$  configurations. In contrast, chiral BINAP is expected to coordinate stereoselectively to either  $\Delta$ - $\text{Eu}(\text{III})$  or  $\Lambda$ - $\text{Eu}(\text{III})$ . As a result, the reversible ligand coordination and dissociation processes promote stereochemical interconversion, leading to a bias of one configuration over the other ( $\Lambda \rightarrow \Delta$ , or *vice versa*), *i.e.*, chirality swapping within the equilibrium system. Thus, the introduction of the chiral ligand shifts the dynamic racemic equilibrium in the preferred direction, effectively generating an asymmetric population of  $\text{Eu}(\text{III})$  species and creating a chiral environment in the excited state.

Subsequently, hydrostatic pressure is applied to the solution systems to evaluate their pressure-dependent optical properties. At 50 and 100 MPa, well-defined PL and CPL spectra are clearly observed, and the (*R*)- and (*S*)-enantiomers maintain their mirror-image relationships (Fig. 2 and Table 1; 50 MPa: red lines; 100 MPa: green lines). These results indicate that the chirality-induced emissive states are preserved even under an applied pressure. As summarised in Table 1, neither the PL emission maxima ( $\lambda_{\text{PL}}$ ) nor CPL maxima ( $\lambda_{\text{CPL}}$ ) of BINAP- $\text{Eu}(\text{III})(\text{hfa})_3$  exhibited significant spectral shifts upon pressurisation. In contrast, the PL and CPL intensities increased significantly at 50 and 100 MPa. This suggests that the pressure-induced shortening of intermolecular distances and compression of the coordination environment influence the energy-transfer efficiency to the  $\text{Eu}(\text{III})$  centre and/or its radiative decay processes. Interestingly, the luminescence dissymmetry

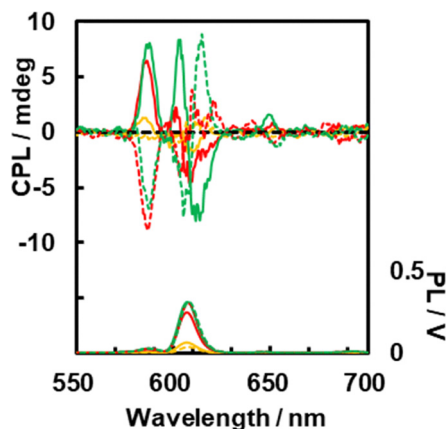


Fig. 2 CPL (top) and PL (bottom) spectra of (*R*)-BINAP- $\text{Eu}(\text{III})(\text{hfa})_3$  (solid lines) and (*S*)-BINAP- $\text{Eu}(\text{III})(\text{hfa})_3$  (dotted lines) in a chloroform solution ( $1.0 \times 10^{-3}$  M). Yellow lines: ambient pressure (0.1 MPa); red lines: hydrostatic pressure (50 MPa); green lines: hydrostatic pressure (100 MPa).

Table 1 Optical properties of chiral BINAP- $\text{Eu}(\text{III})(\text{hfa})_3$  in the  $\text{CHCl}_3$  solution ( $1.0 \times 10^{-3}$  M) under pressure

Pressure (MPa)	$\lambda_{\text{PL}}$ (nm)	$\lambda_{\text{CPL}}$ (nm)	PL Intensity (V)	CPL Intensity (mdeg)	$ g_{\text{CPL}}  \times 10^{-2}$
0.1	692	—	0.0084	—	—
	646	652	0.0011	0.47	6.2
	607	612	0.050	1.6	0.54
	587	599	0.0053	1.2	0.94
		586		0.99	1.3
50	692	—	0.0097	—	—
	646	652	0.0060	0.95	1.8
	607	612	0.27	4.0	0.31
	587	602	0.024	3.1	0.15
		586		7.7	2.2
100	693	—	0.011	—	—
	647	651	0.0066	1.5	2.2
	608	613	0.31	8.4	0.38
	587	604	0.028	8.0	0.26
		588		7.5	1.9



factor  $|g_{\text{CPL}}|$  does not exhibit a uniform response to pressure. Upon the application of 50 MPa, decreases in  $|g_{\text{CPL}}|$  are observed for the bands at  $\lambda_{\text{CPL}} \approx 652, 612,$  and  $599$  nm, whereas an increase in  $|g_{\text{CPL}}|$  is detected near  $586$  nm. Furthermore, slight inverse changes are observed upon increasing the pressure from 50 to 100 MPa. These results indicate that pressure does not simply reinforce the overall chiral ordering but rather exerts transition-dependent effects on individual Eu(III) emissive states.

Hence, emissive excited-state responses differ significantly between ambient (0.1 MPa) and hydrostatic pressures (50 and 100 MPa). Upon pressurisation, the shortening of the BINAP–Eu distance likely increases the energy transfer efficiency to the Eu(III) centre, increasing the PL and CPL intensities. However, the reduction in the ligand–metal distance does not necessarily translate into a more ordered chiral arrangement. Instead, pressure-induced changes in the local symmetry and reorganisation of the excited-state electronic distribution may lead to transition-dependent variations in  $g$ -values. A decrease in the dissymmetry factor is observed for specific emission bands. Thus, we have successfully performed hydrostatic-pressure CPL measurements of chiral BINAP–Eu(III)(hfa)<sub>3</sub> emitters in solution, demonstrating that pressure can serve as a novel external stimulus for the precise modulation of PL and CPL properties.

The BINAP is then replaced with the central chiral ligand QuinoxP to examine the pressure-induced modulation of CPL properties. Chiral (*R,R*)-QuinoxP (or (*S,S*)-QuinoxP) is employed at a concentration of  $1.0 \times 10^{-3}$  M and doped in an equimolar amount into the achiral Eu(III)(hfa)<sub>3</sub> emitter to produce the chiral (*R,R*)-QuinoxP–Eu(III)(hfa)<sub>3</sub> and (*S,S*)-QuinoxP–Eu(III)(hfa)<sub>3</sub> systems. This design enables the evaluation of the influence of differences in the stereochemical structure on the pressure-responsive CPL behaviour by comparing an axially chiral ligand with a centrally chiral ligand. CPL measurements are first performed under ambient pressure (0.1 MPa; yellow lines, Fig. 3 and Fig. S3). Well-defined CPL spectra resulting from the characteristic Eu(III) 4f–4f transitions are clearly observed. Moreover, the spectra obtained for (*R,R*)-QuinoxP and (*S,S*)-QuinoxP exhibit

nearly perfect mirror-image relationships, confirming that the stereochemical information of the chiral ligand has been effectively transferred to the Eu(III) emissive centre.

In the QuinoxP–Eu(III)(hfa)<sub>3</sub> system, CPL emission maxima ( $\lambda_{\text{CPL}}$ ) are observed at approximately 606 and 588 nm, which are assigned to the characteristic Eu(III)  $^5\text{D}_0 \rightarrow ^7\text{F}_J$  transitions. The CPL spectra of (*R,R*)-QuinoxP–Eu(III)(hfa)<sub>3</sub> and (*S,S*)-QuinoxP–Eu(III)(hfa)<sub>3</sub> demonstrate nearly perfect mirror-image relationships and confirm the efficient transfer of the stereochemical information of the central chiral ligand to the Eu(III) emissive centre. The obtained  $|g_{\text{CPL}}|$  values are  $0.55 \times 10^{-2}$  at 606 nm and  $4.6 \times 10^{-2}$  at 588 nm (Fig. 3 and Table 2). The relatively large  $g$ -value at 606 nm suggests that the coordination of QuinoxP effectively perturbs the local symmetry around the Eu(III) centre.

The hydrostatic pressures of 50 and 100 MPa are subsequently applied to the QuinoxP–Eu(III)(hfa)<sub>3</sub> system followed by CPL measurements. For the BINAP–Eu(III)(hfa)<sub>3</sub> system, no significant shifts in the PL or CPL emission maxima are detected under pressurisation, indicating that the electronic energy-level structure of the Eu(III) emissive centre remains essentially unchanged. In contrast, both the PL and CPL intensities increase markedly with increasing pressure.

Notably, the luminescence dissymmetry factor  $|g_{\text{CPL}}|$  exhibits enhancement upon pressurisation. At 100 MPa,  $|g_{\text{CPL}}|$  reaches approximately  $0.84 \times 10^{-2}$  (607 nm) and  $6.4 \times 10^{-2}$  (588 nm), representing a substantial increase compared with the corresponding ambient-pressure values of  $0.55 \times 10^{-2}$  (606 nm) and  $4.6 \times 10^{-2}$  (588 nm). Importantly, the signs of the CPL spectra remained unchanged under pressure, confirming that the absolute chiral configuration was preserved, while the chiroptical response is significantly amplified.

These results demonstrate that, in the optically active emitter QuinoxP–Eu(III)(hfa)<sub>3</sub>, hydrostatic pressure can effectively modulate the excited-state chiroptical response. Although the emission peak positions remain essentially unchanged, the increases in the CPL intensity and  $|g_{\text{CPL}}|$  indicate that pressure influences the excited-state chiral environment and local symmetry around the Eu(III) centre. The  $|g_{\text{CPL}}|$  value increases by approximately 2.2 times, showing continuous enhancement with increasing hydrostatic pressure. This behaviour can be attributed to the pressure-induced shortening of the ligand–metal distance, which improves the efficiency of chirality transfer and promotes the formation of a more effective chiral coordination structure. The observed pressure dependence of  $|g_{\text{CPL}}|$  provides compelling evidence that hydrostatic pressure can directly influence the

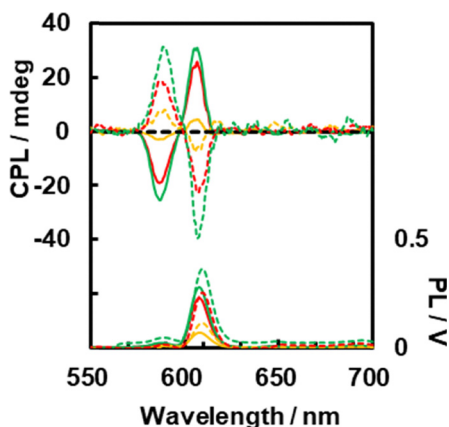


Fig. 3 CPL (top) and PL (bottom) spectra of (*R,R*)-QuinoxP–Eu(III)(hfa)<sub>3</sub> (solid lines) and (*S,S*)-QuinoxP–Eu(III)(hfa)<sub>3</sub> (dotted lines) in a chloroform solution ( $1.0 \times 10^{-3}$  M). Yellow lines: ambient pressure (0.1 MPa); red lines: hydrostatic pressure (50 MPa); green lines: hydrostatic pressure (100 MPa).

Table 2 Optical properties of chiral QuinoxP–Eu(III)(hfa)<sub>3</sub> in a CHCl<sub>3</sub> solution ( $1.0 \times 10^{-3}$  M) under pressure

Pressure (MPa)	$\lambda_{\text{PL}}$ (nm)	$\lambda_{\text{CPL}}$ (nm)	PL intensity (V)	CPL intensity (mdeg)	$ g_{\text{CPL}}  \times 10^{-2}$
0.1	609	606	0.091	6.1	0.55
	589	588	0.0091	5.6	4.6
50	608	607	0.24	24	0.75
	588	586	0.016	19	10
100	608	607	0.32	35	0.84
	588	588	0.034	28	6.4



absolute chiral arrangement of a metal complex and reinforce the excited-state chirality. To the best of our knowledge, this study is the first experimental demonstration of CPL modulation under hydrostatic pressure in a lanthanide Eu-based emitter, revealing a new strategy for CPL control using pressure as an external field.

## Conclusions

This unprecedented study demonstrates that CPL spectra of optically active lanthanide Eu-based emitters, BINAP–Eu(III)(hfa)<sub>3</sub> and QuinoxP–Eu(III)(hfa)<sub>3</sub>, can be measured in solution not only under ambient pressure but also reliably and reproducibly under hydrostatic pressure. It also establishes that pressure leads to a pronounced enhancement of both the CPL intensity and luminescence dissymmetry factor ( $g_{\text{CPL}}$ ). This indicates that the coordination structure of Eu(III) complexes is highly sensitive to pressure and can actively function as an amplification platform for the excited-state chirality. The establishment of a high-pressure CPL measurement system for lanthanide emitters not only provides a new experimental foundation for extreme-environment photonics but also opens a promising avenue for external field-controlled circularly polarised emission devices and pressure-responsive chiroptical materials.

## Conflicts of interest

There are no conflicts to declare.

## Data availability

The data supporting this article are included in the supplementary information (SI). Supplementary information: experimental detail and expanded CPL and PL spectra. See DOI: <https://doi.org/10.1039/d6cp01378c>.

## References

1 E. M. Sánchez-Carnerero, A. R. Agarrabeitia, F. Moreno, B. L. Maroto, G. Muller, M. J. Ortiz and S. de la Moya, *Chemistry*,

- 2015, **21**, 13488–13500; J. Kumar, T. Nakashima and T. Kawai, *J. Phys. Chem. Lett.*, 2015, **6**, 3445–3452; E. Yashima, N. Ousaka, D. Taura, K. Shimomura, T. Ikai and K. Maeda, *Chem. Rev.*, 2016, **116**, 13752–13990; H. Tanaka, Y. Inoue and T. Mori, *ChemPhotoChem*, 2018, **2**, 386–402; J. Han, S. Guo, H. Lu, S. Liu, Q. Zhao and W. Huang, *Adv. Opt. Mater.*, 2018, **6**, 1800538; F. Song, Z. Zhao, Z. Liu, J. W. Y. Lam and B. Z. Tang, *J. Mater. Chem. C*, 2020, **8**, 3284–3301; Y. Sang, J. Han, T. Zhao, P. Duan and M. Liu, *Adv. Mater.*, 2020, **32**, 1900110; G. Albano, G. Pescitelli and L. Di Bari, *Chem. Rev.*, 2020, **120**, 10145–10243; L. E. MacKenzie and R. Pal, *Nat. Rev. Chem.*, 2021, **5**, 109–124; Y. Zhang, S. Yu, B. Han, Y. Zhou, X. Zhang, X. Gao and Z. Tang, *Matter*, 2022, **5**, 837–875.
- 2 G. Muller, *Dalton Trans.*, 2009, 9692–9707; R. Carr, N. H. Evans and D. Parker, *Chem. Soc. Rev.*, 2012, **41**, 7673–7686; J. Kumar, T. Nakashima and T. Kawai, *J. Phys. Chem. Lett.*, 2015, **6**, 3445–3452; Y. Kitagawa, M. Tsurui and Y. Hasegawa, *ACS Omega*, 2020, **5**, 3786–3791; L. E. MacKenzie and R. Pal, *Nat. Rev. Chem.*, 2021, **5**, 109–124; J. Gong and X. Zhang, *Coord. Chem. Rev.*, 2022, **453**, 214329; L. Llanos, P. Cancino, P. Mella, P. Fuentealba and D. Aravena, *Coord. Chem. Rev.*, 2024, **505**, 215675; A. G. Bispo-Jr, N. A. Oliveira, I. M. S. Diogenis and F. A. Sigoli, *Coord. Chem. Rev.*, 2025, **523**, 216279; Y. Zha, Z. Bian and Z. Liu, *Polyhedron*, 2025, **272**, 117452.
- 3 A. Satrijo, S. C. J. Meskers and T. M. Swager, *J. Am. Chem. Soc.*, 2006, **128**, 9030–9031; J. Yuasa, H. Ueno and T. Kawai, *Chem. – Eur. J.*, 2014, **20**, 8621–8627; T. Kimoto, T. Amako, N. Tajima, R. Kuroda, M. Fujiki and Y. Imai, *Asian J. Org. Chem.*, 2013, **2**, 404–410; K. Okano, M. Taguchi, M. Fujiki and T. Yamashita, *Angew. Chem., Int. Ed.*, 2011, **50**, 12474–12477; J. Kumar, T. Nakashima, H. Tsumatori, M. Mori, M. Naito and T. Kawai, *Chem. – Eur. J.*, 2013, **19**, 14090–14097.
- 4 M. E. Sun, F. Wang, M. He, Y. N. Yang, J. K. Yang, M. J. Zhu, Q. Y. Wan, G. Chen, Y. Wang, Y. Fu and Q. Li, *J. Am. Chem. Soc.*, 2025, **147**, 10706–10714.
- 5 J. Ono, H. Sako, N. Fujisawa, M. Kitamatsu, S. Suzuki and Y. Imai, *Chem. Lett.*, 2025, **54**, upaf170.
- 6 K. Mishima, D. Kaji, M. Fujiki and Y. Imai, *ChemPhysChem*, 2021, **22**, 1728–1737.

